The Numerical Solution of Fractional Differential-Algebraic Equations (FDAEs) by Haar Wavelet Functions

Mesut Karabacak, Ercan Çelik

***Abstract*— In this paper, the numerical solution of Fractional Differential-Algebraic Equations (FDAEs) is considered by Haar wavelet functions. We derive the Haar wavelet operational matrix of the fractional order integration and by using it to solve the Fractional Differential-Algebraic Equations. The results obtained are in good-agreement with the exact solutions. It is shown that the technique used here is effective and easy to apply.**

***Index Terms*— differential-algebraic equations (DAEs), fractional differential-algebraic equations (FDAEs), Haar wavelet method, operational matrix**

I. INTRODUCTION

Fractional modeling in differential equations has gained considerable popularity and importance during the past three decades or more. Besides, Differential-Algebraic Equations (DAEs) have been successfully used to characterize for many physical and engineering topics such as polymer physics, fluid flow, electromagnetic theory, dynamics of earthquakes, rheology, viscoelastic materials, viscous damping and seismic analysis. Also differential-algebraic equations with fractional order have been made in some mathematical models in recent times. As known, fractional differential-algebraic equations usually do not have exact solutions. Therefore, approximations and numerical techniques must be used for them and also the solution of these equations has been an attractive subject for many researchers. [1] - [2] - [3] – [4] – [5] – [6] - [7]

In this paper, we want to show by using Haar wavelet functions to solve the fractional order differential-algebraic equations. Firstly, we derive Haar wavelet operational matrix of the fractional order integration and then we use the Haar wavelet operational matrices of the fractional order integration to completely transform the fractional order systems into algebraic systems of equations. Finally, we solve this transformed complicated algebraic equations system by the software Mathematica.

A fractional differential-algebraic equation (FDAE) with the initial conditions is defined as the form below [8]

$$\boldsymbol{D_*^{\alpha_i} x_i(t) = f_i(t, x_1, x_2, \dots x_n, x_1', x_2', \dots x_n')}$$
$$i = 1,2,3, \dots n-1, \quad t \geq 0 \;, 0 < \alpha_i \leq 1$$
$$\boldsymbol{g(t, x_1, x_2, \dots x_n) = 0}$$
$$x_i(0) = \alpha_i \qquad i = 1,2,3, \dots, n \tag{1}$$

Mesut Karabacak, Department of Actuarial Sciences, Faculty of Science, Atatürk University, Erzurum 25240,Turkey

Ercan Çelik, Department of Mathematics, Faculty of Science, Atatürk University, Erzurum 25240, Turkey

II. BASIC DEFINITIONS

There are several definitions of a fractional derivative of order $\alpha > 0$ [9], for example, Riemann-Liouville, Caputo, Grünwald-Letnikov, Hadamard and the generalized functions approach. The most common definitions are Riemann-Liouville and Caputo. We give some basic definitions and properties of fractional calculus theory which are used in this paper.

Definition 2.1. A real function $f(x), x > 0.$ is said to be in the space $C_\mu, \mu \in R$ if there exists a real number $p > \mu$ such that $f(x) = x^P f_I(x)$, where $f_I(x) \in C[0, \infty)$. Clearly, $C_\mu \subset C_\beta$ if $\beta < \mu$.

Definition 2.2. A function $f(x), x < 0.$ is said to be in the space $C_\mu^m, m \in N \cup \{0\}$ if $f^{(m)} \in C_\mu$

Definition 2.3. The Riemann-Liouville fractional integral operator of order $\alpha \geq 0$ of a function, $f \in C_\mu,\ \mu \geq -1$, is defined as

$$I^\alpha f(x) = \frac{1}{\Gamma(\alpha)} \int_0^x (x-t)^{\alpha-1} f(t)dt \,, \alpha > 0, x > 0 \tag{2}$$
$$I^0 f(x) = f(x) \tag{3}$$

The properties of the operator I^α can be found in [10, 11]. We make use of the followings.

For $f \in C_\mu,\ \mu \geq -1,\ \ \alpha, \beta \geq 0$ and $\gamma > -1$

1. $I^\alpha I^\beta f(x) = I^{\alpha+\beta} f(x)$ (4)
2. $I^\alpha I^\beta f(x) = I^\beta I^\alpha f(x)$ (5)
3. $I^\alpha x^\gamma = \frac{\Gamma(\gamma+1)}{\Gamma(\alpha+\gamma+1)} x^{\alpha+\gamma}$ (6)

The Riemann- Liouville fractional derivative has some disadvantages making a model for real-world subjects using fractional differential and fractional differential-algebraic equations. Therefore, we sometimes use a modified fractional differential operator D_*^α introduced by Caputo's work on the theory of viscoelasticity [12].

Definition 2.4. The fractional derivative of $f(x)$ by Caputo is defined as

$$\begin{aligned} D_*^\alpha f(x) &= I^{m-\alpha} D^m f(x) \\ &= \frac{1}{\Gamma(m-\alpha)} \int_0^x (x-t)^{m-\alpha-1} f^{(m)}(t)dt, \end{aligned} \tag{7}$$

for $m-1 < \alpha \leq m,\ m \in N,\ x > 0,\ f \in C_{-1}^m$.
Also, we need here two basic properties.

Lemma 2.1. If $m-1 < \alpha \leq m,\quad m \in N$ and $f \in C_\mu^m, m \geq -1$, then

1. $D_*^\alpha I^\alpha f(x) = f(x)$ (8)
2. $I^\alpha D_*^\alpha f(x) = f(x) - \sum_{k=0}^{m-1} f^{(k)}(0^+) \frac{x^k}{k!},\ \ x > 0.$

(9)

III. Haar Wavelet Operational Matrix of Fractional Order Integration

i. One-dimensional Haar Functions

The scaling function for the family of the Haar wavelets is defined on the interval $[0, 1)$ and is given as below

$$h_n(t) = h_1(2^j t - k),$$
$$n = 2^j + k,\ j \geq 0,\ 0 \leq k \leq 2^j \quad n, j, k \in Z \tag{10}$$

where

$$h_0(t) = 1, \quad 0 \leq t < 1,$$

$$h_1(t) = \begin{cases} 1, & 0 \leq t < 0.5, \\ -1, & 0.5 \leq t < 1 \end{cases} \tag{11}$$

each Haar wavelet h_n has the support $(2^{-j}k,\ 2^{-j}(k+1))$, so that it is zero elsewhere in the interval $[0, 1)$. As might be expected, as n increases, the Haar wavelets become progressively localized. That is, $\{h_n(t)\}$ are like a local basis.

Any function $f(t) \in L_2([0,1])$ have an expansion in Haar series

$$f(t) = \sum_{i=0}^{\infty} c_i h_i(t)$$
$$i = 2^j + k,\ j \geq 0,\ 0 \leq k \leq 2^j \tag{12}$$

where the Haar coefficients c_i, $i = 1,2, \ldots$, are written by

$$c_i = 2^j \int_0^1 f(t) h_i(t) dt \tag{13}$$

which are determined such that the following integral square error ε is minimized

$$\varepsilon = \int_0^1 \left[f(t) - \sum_{i=0}^{m-1} c_i h_i(t) \right]^2 dt,$$
$$m = 2^j,\ j \in \{0\} \cup N \tag{14}$$

By using the orthogonal property of Haar wavelet

$$\int_0^1 h_l(t) h_i(t) dt = \begin{cases} 2^{-j}, & i = l, \\ 0, & i \neq l. \end{cases}$$

The series in Eq. (12) has infinite number of terms. If $f(t)$ is piecewise constant or may be approximated as piecewise constant, then the sum in Eq. (12) may be terminated after m terms, that is [15]

$$f(t) \approx \sum_{i=0}^{m-1} c_i h_i(t) = C_m^T H_m(t) = \hat{f}(t) \tag{15}$$

where $m = 2^j$, T indicates transposition, $\hat{f}(t)$ denotes the truncated sum. The Haar coefficient vector C_m and Haar function vector $H_m(t)$ are defined as

$$C_m \triangleq [c_0, c_1, \ldots, c_{m-1}]^T \tag{16}$$

$$H_m(t) \triangleq [h_0(t), h_1(t), \ldots, h_{m-1}(t)]^T \tag{17}$$

Selecting the collocation points as following

$$t_i = \frac{(2i-1)}{2m},\ i = 1,2, \ldots, m \tag{18}$$

We defined the m-square Haar matrix $\Phi_{m\times m}$ as

$$\Phi_{m\times m} \triangleq \left[H_m\left(\frac{1}{2m}\right) \ H_m\left(\frac{3}{2m}\right) \ \cdots \ H_m\left(\frac{2m-1}{2m}\right) \right] \tag{19}$$

For example, when $m = 8$, the Haar matrix is formed as

$$\Phi_{8\times 8} = \begin{bmatrix} 1 & 1 & 1 & 1 & 1 & 1 & 1 & 1 \\ 1 & 1 & 1 & 1 & -1 & -1 & -1 & -1 \\ 1 & 1 & -1 & -1 & 0 & 0 & 0 & 0 \\ 0 & 0 & 0 & 0 & 1 & 1 & -1 & -1 \\ 1 & -1 & 0 & 0 & 0 & 0 & 0 & 0 \\ 0 & 0 & 1 & -1 & 0 & 0 & 0 & 0 \\ 0 & 0 & 0 & 0 & 1 & -1 & 0 & 0 \\ 0 & 0 & 0 & 0 & 0 & 0 & 1 & -1 \end{bmatrix} \tag{20}$$

Correspondingly, we have

$$\hat{f}_m = \left[\hat{f}\left(\frac{1}{2m}\right) \ \hat{f}\left(\frac{3}{2m}\right) \cdots \hat{f}\left(\frac{2m-1}{2m}\right) \right] = C_m^T \Phi_{m\times m} \tag{21}$$

Because the m-dimensional Haar matrix $\Phi_{m\times m}$ is an invertible matrix, the Haar coefficient vector C_m^T can be obtained by [13]

$$C_m^T = \hat{f}_m \Phi^{-1}{}_{m\times m} \tag{22}$$

ii Operational matrix of the fractional order integration

The integration of the $H_m(t)$ defined in Eq. (17) can be approximated by Haar series with Haar coefficient matrix P [16].

$$\int_0^t H_m(\tau) d\tau \approx \mathrm{P}_{m\times m} H_m(t) \tag{23}$$

where the m-square matrix P is called the Haar wavelet operational matrix of integration [14]. Our goal is to derive the Haar wavelet operational matrix of the fractional order integration. For this goal, we use the definition of Riemann–Liouville fractional order integration, as below [13]

$$(I^\alpha f)(t) = \frac{1}{\Gamma(\alpha)} \int_0^t (1-t)^{\alpha-1} f(\tau) d\tau = \frac{1}{\Gamma(\alpha)} t^{\alpha-1} * f(t) \tag{24}$$

where $t^{\alpha-1} * f(t)$ denotes convolution product. Now if $f(t)$ is expanded in Haar functions, as shown in Eq. (15), the Riemann–Liouville fractional integration becomes

$$(I^\alpha f)(t) = \frac{1}{\Gamma(\alpha)} t^{\alpha-1} * f(t) \approx C_m^T \frac{1}{\Gamma(\alpha)} \{t^{\alpha-1} * H_m(t)\} \tag{25}$$

Thus if $t^{\alpha-1} * f(t)$ can be integrated, then expanded in Haar functions, the Riemann-Liouville fractional order integration is solved by the Haar functions.

However, we can define a m −set of Block Pulse Functions (BPFs) as

$$b_i(t) = \begin{cases} 1, & 1/m \leq t < (1+m)/m, \\ 0, & \text{otherwise} \end{cases} \tag{26}$$

where $i = 0,1,2,\cdots,(m-1)$

$b_i(t)$ functions have some useful properties like disjointness and orthogonality. Respectively that is,

$$b_i(t)b_l(t) = \begin{cases} 0, & i \neq l \\ b_i(t), & i = l \end{cases} \tag{27}$$

$$\int_0^1 b_i(\tau)b_l(\tau)d\tau = \begin{cases} 0, & i \neq l \\ 1/m, & i = l \end{cases} \tag{28}$$

As seen the Haar functions are piecewise constant, and so it can be transformed into an m-term block pulse functions (BPF) as

$$H_m(t) = \Phi_{m\times m} B_m(t) \tag{29}$$

where

$$B_m(t) \triangleq [b_0(t) \;\; b_0(t) \;\; \cdots \;\; b_i(t) \cdots b_{m-1}(t)]^T \tag{30}$$

Kilicman and Al Zhour [15], have introduced the Block Pulse operational matrix of the fractional order integration F^α as follows

$$(I^\alpha B_m)(t) \approx F^\alpha B_m(t) \tag{31}$$

where

$$F^\alpha = \frac{1}{m^\alpha}\frac{1}{\Gamma(\alpha+2)}\begin{bmatrix} 1 & \xi_1 & \xi_2 & \cdots & \xi_{m-1} \\ 0 & 1 & \xi_1 & \cdots & \xi_{m-2} \\ 0 & 0 & 1 & \cdots & \xi_{m-3} \\ \\ 0 & 0 & 0 & \ddots & \vdots \\ 0 & 0 & 0 & 0 & 1 \end{bmatrix} \tag{32}$$

$$\text{with } \xi_k = (k+1)^{\alpha+1} - 2k^{\alpha+1} + (k-1)^{\alpha+1} \tag{33}$$

Next, we derive the Haar wavelet operational matrix of the fractional order integration.
Let

$$(I^\alpha H_m)(t) \approx P^\alpha_{m\times m} \mathrm{H_m(t)} \tag{34}$$

where the $m-$ square matrix $P^\alpha_{m\times m}$ is called the Haar wavelet operational matrix of the fractional order integration. Using Eqs. (29)(30) and (31), we get

$$(I^\alpha H_m)(t) \approx (I^\alpha \Phi_{\mathrm{m\times m}} B_m)(t) = \Phi_{\mathrm{m\times m}}(I^\alpha B_m)(t) \approx \Phi_{\mathrm{m\times m}} F^\alpha B_m(t) \tag{35}$$

from Eqs. (34) and (35) we get

$$P^\alpha_{m\times m} H_m(t) = P^\alpha_{m\times m}\Phi_{\mathrm{m\times m}} B_m(t) = \Phi_{\mathrm{m\times m}} F^\alpha B_m(t) \tag{36}$$

Then, the Haar wavelet operational matrix of the fractional order integration $P^\alpha_{m\times m}$ is written by

$$P^\alpha_{m\times m} = \Phi_{\mathrm{m\times m}} F^\alpha \Phi^{-1}_{\mathrm{m\times m}} \tag{37}$$

For example, $\alpha = 0.5$ and $m = 8$, the operational matrix $P^\alpha_{m\times m}$ is computed below [15]

$$P^{0.5}_{8\times8} = \begin{bmatrix} 0.7523 & -0.2203 & -0.1558 & -0.0820 & -0.1102 & -0.0580 & -0.0447 & -0.0377 \\ 0.2203 & 0.3116 & -0.1558 & 0.2296 & -0.1102 & -0.0580 & 0.1756 & 0.0782 \\ 0.0410 & 0.1148 & 0.2203 & -0.0350 & -0.1102 & 0.1623 & -0.0389 & -0.0063 \\ 0.0779 & -0.0779 & 0 & 0.2203 & 0 & 0 & -0.1102 & 0.1623 \\ 0.0094 & 0.0196 & 0.0812 & -0.0032 & 0.1558 & -0.0247 & -0.0026 & -0.0009 \\ 0.0112 & 0.0439 & -0.0551 & -0.0194 & 0 & 0.1558 & -0.0247 & -0.0026 \\ 0.0145 & -0.0145 & 0 & 0.0812 & 0 & 0 & 0.1558 & -0.0247 \\ 0.0275 & -0.0275 & 0 & -0.0551 & 0 & 0 & 0 & 0.1558 \end{bmatrix}$$

IV. NUMERICAL APPLICATIONS

Showing the efficiency of the method, we consider the following fractional differential-algebraic equations. All the numerical results were obtained by using the software Mathematica 10.0

Example 4.1. We consider the following fractional -algebraic equation.

$$0 < \alpha \leq 1$$

$$\begin{gathered} D^\alpha x(t) - tDy(t) + x(t) - (1+t)y(t) = 0 \\ y(t) - sint = 0 \end{gathered} \tag{38}$$

with initial conditions $x(0) = 1,\; y(0) = 0$ and exact solutions $x(t) = e^{-t} + tsint,\; y(t) = sint$
when $\alpha = 1$
Now, we redesign all terms of the equation with Haar series form below. Firstly, let

$$Dx(t) = R^T H_m(t) \tag{39}$$

and

$$Dy(t) = K^T H_m(t) \tag{40}$$

with the initial states, we get

$$D^\alpha x(t) = R^T P^{1-\alpha}_{m\times m} H_m(t) \tag{41}$$

$$x(t) = R^T P^1_{m\times m} H_m(t) + \underbrace{1}_{x(0)} \tag{42}$$

$$y(t) = K^T P^1_{m\times m} H_m(t) + \underbrace{0}_{y(0)} \tag{43}$$

Similarly, $f(t) = \sin t$ can be expanded by the Haar functions below

$$f(t) = f_m^T H_m(t) = [\sin t]_{\mathrm{haar}} \tag{44}$$

Substituting Eqs. (40-41-42-43-44) into (38), we get

$$\begin{gathered} R^T P^{1-\alpha}_{m\times m} H_m(t) - tK^T H_m(t) + R^T P^1_{m\times m} H_m(t) + 1 \\ - (1+t)K^T P^1_{m\times m} H_m(t) = 0 \\ \\ K^T P^1_{m\times m} H_m(t) - [\sin t]_{\mathrm{haar}} = 0 \end{gathered} \tag{45}$$

Hereby, Eq. (38) has been transformed into a system of algebraic equations. Substituting values and solving the algebraic equations system, we can find the coefficients R_m^T . Then using Eq. (42), we can get $x(t)$. The numerical results for $m = 8, 32, 128$ are shown in Table 1,2,3 and Fig 1,2,3. The numerical solution is in good agreement with the exact solutions.

Table 1. Comparison of the numerical values of $x(t)$ for m = 8

m = 8	∝=0.25	∝=0.5	∝=0.75	∝=1		
t	$x(t)$	$x(t)$	$x(t)$	$x(t)$	$x_{exact}(t)$	$x_{error}(t)$
t=0	0.718159	0.834216	0.907282	0.948749	1.	0.0512505
t=0.1	0.718159	0.834216	0.907282	0.948749	0.914821	0.0339287
t=0.2	0.686364	0.729621	0.802391	0.868562	0.858465	0.0100972
t=0.3	0.841455	0.805047	0.800684	0.831463	0.829474	0.00198882
t=0.4	0.920544	0.876959	0.841859	0.834009	0.826087	0.0079216
t=0.5	1.08287	0.989918	0.917579	0.872034	0.846243	0.0257907
t=0.6	1.08287	0.989918	0.917579	0.872034	0.887597	0.015563
t=0.7	1.19744	1.11038	1.01788	0.940697	0.947538	0.0068404
t=0.8	1.34758	1.24052	1.13501	1.03455	1.02321	0.0113343
t=0.9	1.46242	1.36971	1.26177	1.14762	1.11156	0.0360512

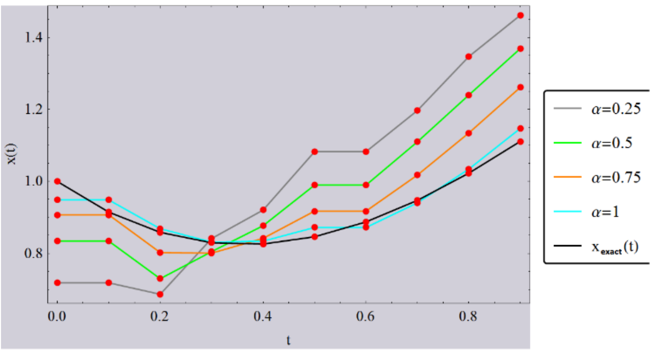

Fig 1. The graph of $x(t)$ for different values of α for $m = 8$

Table 2. Comparison of the numerical values of $x(t)$ for m = 32

m=32	∝=0.25	∝=0.5	∝=0.75	∝=1		
t	$x(t)$	$x(t)$	$x(t)$	$x(t)$	$x_{exact}(t)$	$x_{error}(t)$
t=0	0.755277	0.898167	0.960868	0.9851	1.	0.0149001
t=0.1	0.668525	0.758682	0.842397	0.908652	0.914821	0.00616903
t=0.2	0.734891	0.755093	0.801024	0.857432	0.858465	0.00103258
t=0.3	0.80229	0.788708	0.79753	0.830224	0.829474	0.000749809
t=0.4	0.891566	0.845801	0.821455	0.825576	0.826087	0.000511798
t=0.5	1.01993	0.946003	0.88577	0.851529	0.846243	0.00528577
t=0.6	1.12119	1.03327	0.952761	0.892594	0.887597	0.00499712
t=0.7	1.22366	1.12698	1.03187	0.949773	0.947538	0.00223485
t=0.8	1.32443	1.22407	1.1199	1.0207	1.02321	0.00251104
t=0.9	1.42115	1.3217	1.21382	1.10286	1.11156	0.00870196

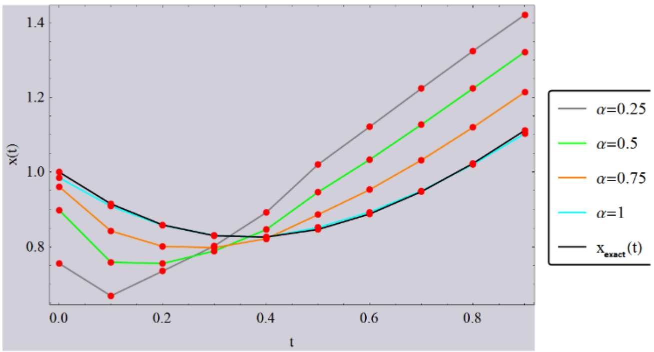

Fig 2. The graph of $x(t)$ for different values of α for $m = 32$

Table 3. Comparison of the numerical values of $x(t)$ for m = 128

m=128	∝=0.25	∝=0.5	∝=0.75	∝=1		
t	$x(t)$	$x(t)$	$x(t)$	$x(t)$	$x_{exact}(t)$	$x_{error}(t)$
t=0	0.808558	0.944945	0.985447	0.996139	1.	0.00386059
t=0.1	0.679012	0.76541	0.851144	0.916502	0.914821	0.00168166
t=0.2	0.727777	0.754367	0.80185	0.858814	0.858465	0.000349671
t=0.3	0.807262	0.790713	0.798005	0.829366	0.829474	0.000108214
t=0.4	0.90261	0.854189	0.826033	0.826312	0.826087	0.000224122
t=0.5	1.00732	0.935718	0.87841	0.847487	0.846243	0.00124384
t=0.6	1.10845	1.02195	0.943653	0.886413	0.887597	0.00118456
t=0.7	1.2194	1.12299	1.02838	0.94701	0.947538	0.000527254
t=0.8	1.32856	1.22814	1.12372	1.02386	1.02321	0.000649027
t=0.9	1.43283	1.33381	1.22584	1.11376	1.11156	0.00219866

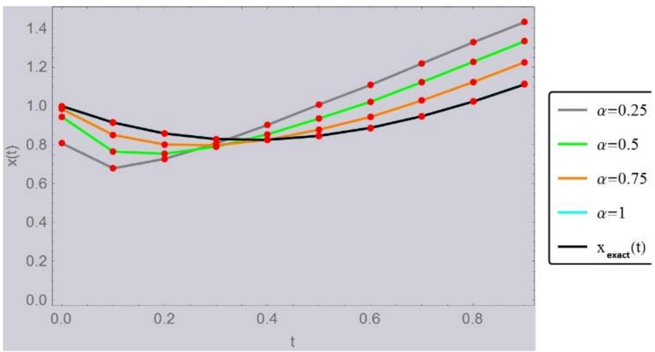

Fig 3. The graph of $x(t)$ for different values of α for $m = 128$

Example 4.2. We consider the following fractional differential-algebraic equation.

$$
\begin{aligned}
D^{\alpha}x(t) + x(t) - y(t) &= -sint \\
x(t) + y(t) &= e^{-t} + sint \\
0 < \alpha &\leq 1
\end{aligned}
\tag{46}
$$

with initial conditions $x(0) = 1,\ y(0) = 0$ and exact solutions $x(t) = e^{-t}$ and $y(t) = sint$ when $\alpha = 1$

Now, let

$$Dx(t) = U^T H_m(t) \tag{47}$$

and

$$Dy(t) = V^T H_m(t) \tag{48}$$

with the initial states, we get

$$D^{\alpha} x(t) = U^T P^{1-\alpha}_{m\times m} H_m(t) \tag{49}$$

$$x(t) = U^T P^{1}_{m\times m} H_m(t) + \underbrace{1}_{x(0)} \tag{50}$$

$$y(t) = V^T P^{1}_{m\times m} H_m(t) + \underbrace{0}_{y(0)} \tag{51}$$

Similarly,

$$j(t) = -sint$$

and

$$n(t) = e^{-t} + sint$$

can be expanded by the Haar functions below

$$j(t) = j_m^T H_m(t) = [-\sin t]_{haar}$$
$$,\ n(t) = n_m^T H_m(t) = [e^{-t} + \sin t]_{haar} \tag{52}$$

Substituting Eqs. (48-49-50-51-52) into (46), we get

$$U^T P^{1-\alpha}_{m\times m} H_m(t) + U^T P^{1}_{m\times m} H_m(t) + 1 - V^T P^{1}_{m\times m} H_m(t) + [\sin t]_{haar} = 0$$

$$U^T P^{1}_{m\times m} H_m(t) + 1 + V^T P^{1}_{m\times m} H_m(t) - [e^{-t} + \sin t]_{haar} = 0$$

(53)

Hence, Eq. (46) has been transformed into an algebraic equations system. Solving this system, we can find the coefficients U_m^T . Then using Eq. (50), we can get $x(t)$. The numerical results for $m = 8,32,128$ are shown in Table 4,5,6 and Fig 4,5,6 for $x(t)$ and by same way for $y(t)$ are shown in Table 7,8,9. and Fig 7,8,9. The numerical solution is in good agreement with the exact solutions.

Table 4. Comparison of the numerical values of $x(t)$ for m = 8

m = 8	∝=0.25	∝=0.5	∝=0.75	∝=1		
t	$x(t)$	$x(t)$	$x(t)$	$x(t)$	$x_{exact}(t)$	$x_{error}(t)$
t=0	0.740771	0.830452	0.89799	0.941079	1.	0.0589215
t=0.1	0.740771	0.830452	0.89799	0.941079	0.904837	0.0362411
t=0.2	0.629461	0.677678	0.753775	0.830197	0.818731	0.011466
t=0.3	0.620348	0.642125	0.673724	0.732411	0.740818	0.00840716
t=0.4	0.552602	0.578078	0.605185	0.646168	0.67032	0.0241523
t=0.5	0.541898	0.540616	0.547911	0.570099	0.606531	0.0364318
t=0.6	0.541898	0.540616	0.547911	0.570099	0.548812	0.0212872
t=0.7	0.494188	0.499459	0.498046	0.503	0.496585	0.00641461
t=0.8	0.481892	0.466772	0.454117	0.44381	0.449329	0.00551909
t=0.9	0.447091	0.435622	0.415053	0.391594	0.40657	0.0149757

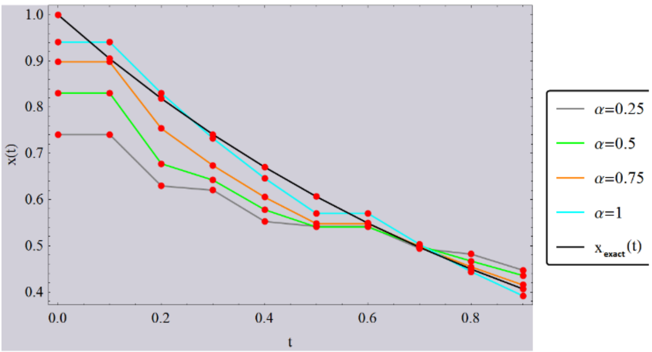

Fig 4. The graph of $x(t)$ for different values of α for $m = 8$

Table 5. Comparison of the numerical values of $y(t)$ for m = 8

m = 8	∝=0.25	∝=0.5	∝=0.75	∝=1		
t	$y(t)$	$y(t)$	$y(t)$	$y(t)$	$y_{TAM}(t)$	$y_{HATA}(t)$
t=0	0.261101	0.17142	0.103883	0.060793	0.	0.0607939
t=0.1	0.261101	0.17142	0.103883	0.060793	0.099833	0.0390395
t=0.2	0.385971	0.337755	0.261658	0.185236	0.198669	0.0134337
t=0.3	0.418706	0.396929	0.36533	0.306643	0.29552	0.0111229
t=0.4	0.516723	0.491247	0.46414	0.423157	0.389418	0.0337387
t=0.5	0.561187	0.56247	0.555174	0.532987	0.479426	0.0535611
t=0.6	0.561187	0.56247	0.555174	0.532987	0.564642	0.0316558
t=0.7	0.643251	0.637979	0.639393	0.634439	0.644218	0.0097789
t=0.8	0.687864	0.702984	0.715639	0.725946	0.717356	0.0085900
t=0.9	0.750595	0.762064	0.782634	0.806093	0.783327	0.0227659

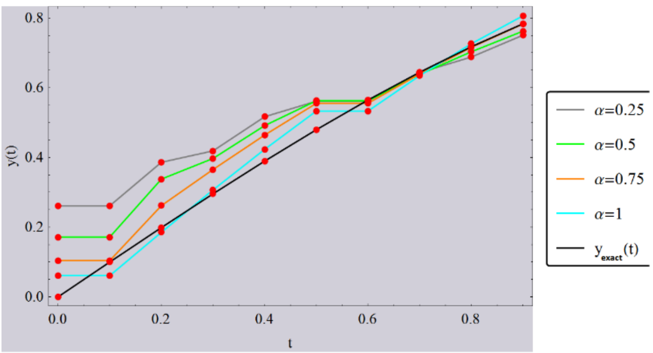

Fig 5. The graph of $y(t)$ for different values of α for $m = 8$

Table 6. Comparison of the numerical values of $x(t)$ for m=32

m = 32	∝=0.25	∝=0.5	∝=0.75	∝=1		
t	$x(t)$	$x(t)$	$x(t)$	$x(t)$	$x_{exact}(t)$	$x_{error}(t)$
t=0	0.795161	0.903384	0.960563	0.984614	1.	0.0153864
t=0.1	0.676905	0.75091	0.827633	0.896485	0.904837	0.00835263
t=0.2	0.648953	0.689144	0.747001	0.816245	0.818731	0.0024854
t=0.3	0.607608	0.641041	0.683477	0.743189	0.740818	0.00237058
t=0.4	0.580252	0.600786	0.629933	0.676672	0.67032	0.0063519
t=0.5	0.544298	0.554566	0.568868	0.597151	0.606531	0.00937943
t=0.6	0.520223	0.523946	0.528777	0.543706	0.548812	0.00510517
t=0.7	0.498754	0.496064	0.492542	0.495045	0.496585	0.00153984
t=0.8	0.478835	0.47051	0.459554	0.45074	0.449329	0.001411
t=0.9	0.460617	0.446988	0.429373	0.4104	0.40657	0.00383038

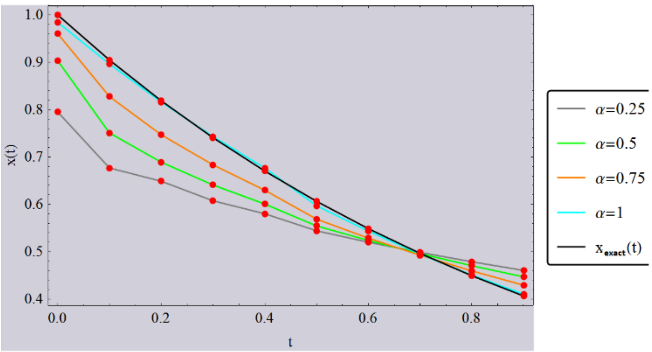

Fig 6. The graph of $x(t)$ for different values of α for $m = 32$

Table 7. Comparison of the numerical values of $y(t)$ for m = 32

m = 32	∝=0.25	∝=0.5	∝=0.75	∝=1		
t	$y(t)$	$y(t)$	$y(t)$	$y(t)$	$y_{TAM}(t)$	$y_{HATA}(t)$
t=0	0.20496	0.0967363	0.039558	0.0155072	0.	0.0155072
t=0.1	0.328647	0.254642	0.177918	0.109066	0.0998334	0.0092330
t=0.2	0.368954	0.328763	0.270906	0.201662	0.198669	0.0029925
t=0.3	0.428062	0.39463	0.352194	0.292481	0.29552	0.0030387
t=0.4	0.477148	0.456614	0.427467	0.380728	0.389418	0.0086900
t=0.5	0.545908	0.53564	0.521338	0.493055	0.479426	0.0136292
t=0.6	0.595822	0.5921	0.587269	0.572339	0.564642	0.0076967
t=0.7	0.642886	0.645576	0.649099	0.646595	0.644218	0.0023774
t=0.8	0.687076	0.695401	0.706357	0.715171	0.717356	0.0021853
t=0.9	0.727248	0.740876	0.758491	0.777464	0.783327	0.0058628

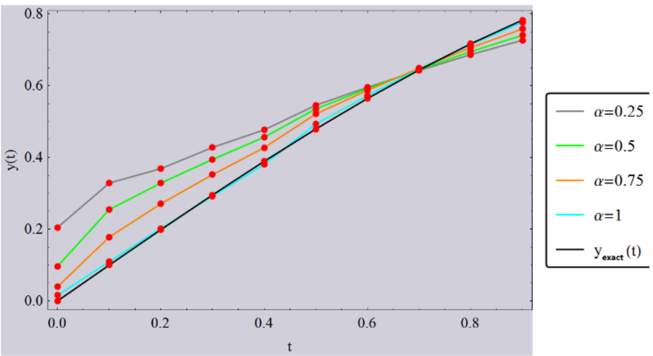

Fig 7. The graph of $y(t)$ for different values of α for $m = 32$

Table 8. Comparison of the numerical values of $x(t)$ for m = 128

m = 128	∝=0.25	∝=0.5	∝=0.75	∝=1		
t	$x(t)$	$x(t)$	$x(t)$	$x(t)$	$x_{exact}(t)$	$x_{error}(t)$
t=0	0.837625	0.947223	0.985487	0.996108	1.	0.003891
t=0.1	0.694830	0.762959	0.839847	0.906966	0.904837	0.002129
t=0.2	0.645960	0.691372	0.750024	0.819375	0.818731	0.000644
t=0.3	0.608269	0.639287	0.681130	0.740242	0.740818	0.000575
t=0.4	0.575881	0.596161	0.623803	0.668753	0.67032	0.001566
t=0.5	0.547148	0.558630	0.574218	0.604167	0.606531	0.002363
t=0.6	0.523189	0.527625	0.533584	0.550100	0.548812	0.001288
t=0.7	0.499571	0.497186	0.494000	0.496974	0.496585	0.000388
t=0.8	0.478068	0.469498	0.458257	0.448978	0.449329	0.000350
t=0.9	0.458432	0.444184	0.425791	0.405617	0.40657	0.000951

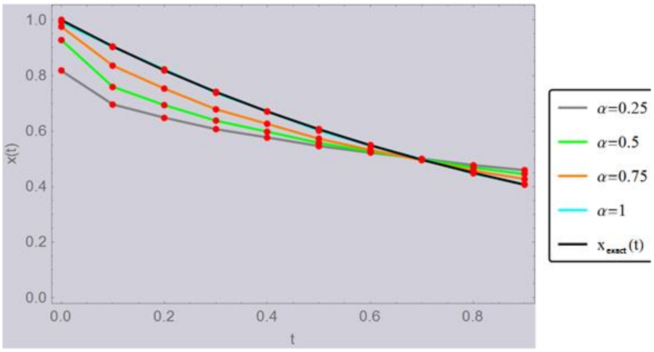

Fig 8. The graph of $x(t)$ for different values of α for $m = 128$

Table 9. Comparison of the numerical values of $y(t)$ for m = 128

m = 128	∝=0.25	∝=0.5	∝=0.75	∝=1		
t	$y(t)$	$y(t)$	$y(t)$	$y(t)$	$y_{TAM}(t)$	$y_{HATA}(t)$
t=0	0.162382	0.052784	0.01452	0.0038986	0.	0.00389869
t=0.1	0.309632	0.241502	0.164614	0.0974953	0.099833	0.00233816
t=0.2	0.371313	0.325902	0.26725	0.197899	0.198669	0.00077010
t=0.3	0.428237	0.397219	0.355376	0.296263	0.29552	0.00074306
t=0.4	0.484445	0.464165	0.436523	0.391574	0.389418	0.00215538
t=0.5	0.539867	0.528386	0.512797	0.482848	0.479426	0.00342282
t=0.6	0.589617	0.58518	0.579222	0.562705	0.564642	0.00193698
t=0.7	0.641022	0.643407	0.646593	0.643619	0.644218	0.00059834
t=0.8	0.68881	0.69738	0.708621	0.7179	0.717356	0.00054380
t=0.9	0.731967	0.746215	0.764608	0.784782	0.783327	0.00145472

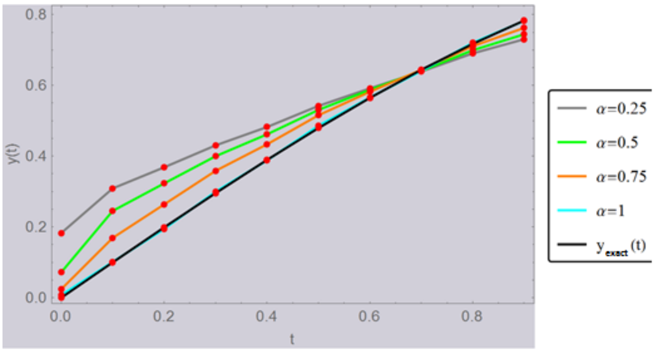

Fig 9. The graph of $y(t)$ for different values of α for $m = 128$

V. Conclusion

In this paper, the Haar wavelet functions has been extended to solve fractional differential-algebraic equations (FDAEs). The results obtained by the method are in good agreement with the given exact solutions. The study show that the method is effective techniques to solve fractional differential–algebraic equations, and the method presents real advantages in terms of comprehensible applicability and precision

Acknowledgements:

This work was supported by Scientific Research Projects (BAP) commission of the Atatürk University. Project Number: 2011/85

REFERENCES

[1] Mainardi F. Fractional calculus: Some basic problems in continuum and statistical mechanics, in: A. Carpinteri, F. Mainardi (Eds.), Fractals and Fractional Calculus in Continuum Mechanics, Springer, NewYork, 1997, pp.291-348.

[2] Carpinteri A, F Mainardi F. Fractals and Fractional Calculus in Continuum Mechanics, Springer Verlag, Wien, NewYork, 1997

[3] İbiş B. Bayram M. Numerical comparison of methods for solving fractional differential-algebraic equations (FDAEs), Computers and Mathematics with Applications 62 (2011) 3270-3278

[4] Karabacak M, Çelik E. The numerical solution of fractional differential-algebraic equations (FDAEs), New Trends in Mathematical Sciences, Vol.1 No.1 (2013), pp 106.

[5] Yiğider M, Çelik E. The numerical solution of partial differential-algebraic equations , Advances in Difference Equations (2013) 2013:8

[6] Khodadadi,E and Karabacak, M Solving fuzzy fractional partial differential equations by fuzzy Laplace-Fourier transforms. Journal of Computational Analysis and Applications, Vol. 19, No.2, pp.260-271, Eudoxus Press LLC, 2015

[7] Turut V, Çelik E, Yiğider M. Multivariate padé approximation for solving partial differential equations (PDE), International Journal for Numerical Methods in Fluids, vol 66, (2011) 1159-1173.

[8] Zurigat M, Momani S, Alawneh A. Analytical approximate solutions of systems of fractional algebraic–differential equations by homotopy analysis method, Comput. Math. Appl. 59 (3) (2010) 1227–1235.

[9] Podlubny I. Fractional Differential Equations. An Introduction to Fractional Derivatives Fractional Differential Equations Some Methods of their Solution and Some of their Applications, Academic Press, San Diego, 1999.

[10] Miller KS, Ross B. An Introduction to the Fractional Calculus and Fractional Differential Equations, John Wiley and Sons Inc., New York, 1993.

[11] Oldham K. Spanier, J. The Fractional Calculus, Academic Press, New York, 1974.

[12] Caputo M. Linear models of dissipation whose Q is almost frequency independent part II, J. Roy. Aust. Soc. 13 (1967) 529-539.

[13] Li Y, Zhao W. Haar wavelet operational matrix of fractional order integration and its applications in solving the fractional order differential equations, Appl. Math. Comput. 216 (2010) 2276–2285.

[14] Chen C, Hsiao C. Haar wavelet method for solving lumped and distributed-parameter systems, IEE P.-Contr. Theor. Ap. 144 (1997) 87–94.

[15] Kilicman A, Al Zhour ZAA. Kronecker operational matrices for fractional calculus and some applications, Appl. Math. Comput. 187 (2007) 250–265